Computer Simulation of Airflow Distribution in a Heat Pump Dryer

Kavindi M. A. R.[1*], Amaratunga K.S.P.[1], Ekanayake E.M.A.C[2]

[1]*Department of Agricultural Engineering, Faculty of Agriculture, University of Peradeniya, Sri Lanka.*
[2]*Postgraduate Institute of Agriculture, University of Peradeniya, Sri Lanka.*

***Abstract*: Computer simulation is an effective technique for better understanding the physical phenomena of drying. Understanding and predicting the drying behavior before applying the material would increase the dryer efficiency by properly designing existing heat pump dryer systems. This study was done to simulate the airflow in a heat pump dryer chamber using Computational Fluid Dynamics (CFD). COMSOL Multiphysics software v5.4 has been used for simulation. Air velocity, temperature, and relative humidity distribution profile were achieved by solving the Naiver stoke fluid equation, Heat transfer equation, and Transport of diluted species equation (Fick's law). The simulated data for nine different locations were verified using experimental results. The relative error and mean relative deviation for temperature profile were less than ±1.8% and 7.8%. It was recorded less than ±2.8% and 10.6% values for the relative error and mean relative deviation for relative humidity profiles. Therefore, this would be a suitable prediction method to understand the airflow pattern and conditions inside a chamber**

***Keywords*: COMSOL Multiphysics, Computational Fluid Dynamics (CFD), Computer Simulation, Heat Pump Dryings**

I. INTRODUCTION

Even though drying is very essential operation in food industries, it consumes large amounts of energy and time. Any improvement in the existing dryer design will reduce the cost and energy, improve the quality of dried products, and be beneficial for the industry. The development of a heat pump dryer is advantageous due to it provide huge savings for industry. Researchers have proven that compare to other drying methods, it facilitates higher energy efficiency, better product quality, the ability to operate independently of outside ambient weather conditions, environmentally friendly drying condition [7, 9, 15, 21, 24]. In the drying process, drying air temperature, humidity, and velocity are the main factors that affect the product's drying rate [8, 19].

In deep bed dryers, heat and mass transfer phenomena involve over-drying in the lower zone and under-drying in the upper zone [22]. Therefore, in designing suitable geometric configurations of the drying chamber, predicting the airflow velocity, temperature, and relative humidity inside the dryer helps to optimize the design and improve the drying process before the actual dryer is built [19]. Mathematical modelling has been used to model the airflow behavior inside several kinds of dryers [4, 11, 16]. However, Mathematical modelling is complicated process and need a developed technology to solve the complex formulations.

Computational Fluid Dynamics (CFD) modelling and simulation is a widely accepted technique for mathematical modelling. Woo has described that the CFD approach is the cost-effective innovative solution for design and development of drying equipment [25]. With the advancement of computer power and numerical methods, it can easily predict airflow behavior with the variables of velocity, temperature, moisture content, kinetic energy etc. [2-3, 5-6, 9, 14, 18, 22, 26]. Most of researchers have discussed several applications of CFD simulation in drying systems including with the different configurations, different drying conditions, for several drying materials etc. [10, 22-23]. Furthermore, they have discussed future improvements and needs of CFD modelling and simulation.

Especially for large-scale dryers, measuring drying parameters are difficult since several sensors need to be place at various locations and directions. Due to it is a costly and time-consuming operation CFD software may be used to predict. The simulation results need to be compared with actual drying results and when there is an agreement of accuracy, it may be applied for other drying systems and many researchers has been proved this method [2-3, 5, 10, 14, 18-19, 22-23].

In this study, an industrial scale heat pump-based empty dryer was used for the experiment. COMSOL Multiphysics software was used for the simulation; Turbulent k-ε model, Heat transfer model and transport of diluted species in fluid model were used for simulation of velocity, temperature, and relative humidity profile, respectively. 3D geometry of the chamber and its physical properties, considered during the simulation, was taken from a specific experiment conducted in an industry. The performance of simulations was compared with experimental data. This study will develop a CFD simulation model for the airflow, temperature, and relative humidity distribution inside the heat pump-based drying chamber.

II. MODEL DEVELOPMENT

A. Experimental setup

The industrial-scale heat pump dryer was used in this study for the experiment at the Helabima Food Pvt (Ltd), Namalthenna, Kandy, Sri Lanka. As shown in Fig.1, the system consisted of two major parts: the heat pump unit and the drying chamber. It consisted of an evaporator, condenser, compressor, expansion valve, and blower to provide the required airflow to the drying system. The evaporator

absorbed heat from the ambient air and produce low moist, cold air. The evaporated moisture from the air is removed to the environment through the opening at the evaporator unit. At the condenser unit, the heat exchanger transferred the heat from the refrigerant into the air, and the blower will produce an airflow with a speed of 39.85 ms^{-1} into the drying chamber. The drying chamber was in cylindrical shape with a height of 1.2 m, a diameter of 0.95 m, and made of stainless steel with a thickness of 0.002 m. The inlet diameter of the drying chamber was 0.13 m [13].

Fig. 1 Schematic diagram of Heat Pump dryer [13]

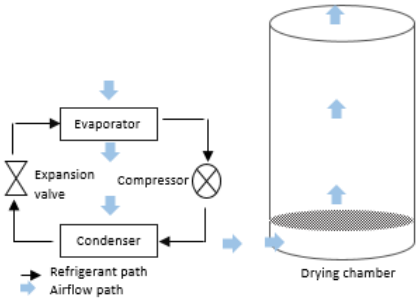

The temperature and the relative humidity were measured using AM2302 (wired DHT22) sensors installed at inlet, outlet and nine locations (Fig. 2) in three different layer depths at the left side, assuming that values from other sides are the same. Sensors were installed form 15cm, 45cm and 75cm depth layer below from top of the chamber. Inlet air velocity was measured using a portable velocity meter (KURZ instruments, 440 series, Chatsworth, California.). The outlet velocity was measured using a Davis vane anemometer (Davis Instruments, A/2-4 in. standard model, Davis Instrument Mfg. Co., Baltimore, Md.).

Fig.2 Sensor positions in the drying chamber [13]

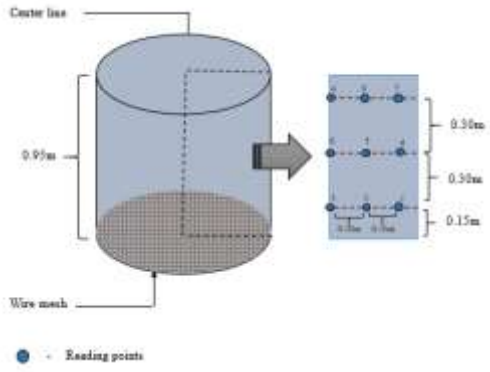

B. CFD Simulation

Governing equations of fluid flow and heat transfer were considered mathematical formulations of the conservation laws of fluid mechanics and are referred to as the Navier-Stokes equations. In COMSOL Multiphysics, the resulting equations were written as below:

1) Turbulent k-ε Model $\frac{\partial \rho}{\partial t} + \nabla.(\rho u) = 0$ (1)

$$\rho \frac{\partial u}{\partial t} + \rho(u.\nabla)u = \nabla.[-pI + \mu(\nabla u + (\nabla u)^T)] + F \quad (2)$$

2) Heat Transfer in Fluid

$$\rho c_p \left(\frac{\partial T}{\partial t} + U.\nabla T\right) + \nabla.q = Q + Q_p + Q_{vd} \quad (3)$$

The second term (Eq. 4) of the right-hand side is the work done by pressure changes and results from heating under adiabatic compression and some thermoacoustic effects. It is generally small for low match number flows.

$$Q_p = \alpha_p T \left(\frac{\partial P}{\partial t} + u.\nabla p\right) \quad (4)$$

The third term (Eq. 5) represents viscous dissipation in the fluid.

$$Q_{vd} = \tau : \nabla u \quad (5)$$

3) Diluted species transport in fluid

This interface can be found under the chemical species transport branch used to calculate the concentration field of a diluted solvent. Transport and reaction of species in a gas, liquid, or solid can be handled. The main force for the transport phenomena is diffusion by Fick's law.

$$\frac{\vartheta c}{\vartheta t} = D\partial^2 C/\partial x^2 \quad (6)$$

Mainly simulation was conducted based on the following two steps: stationary fluid flow study using single-phase turbulent k-ε model; Time-dependent study with fully coupled heat and moisture transfer model. The CFD simulation was carried out for half of the dryer, considering the axisymmetric chamber to save the computational time and avoid the complexity. The initial and boundary condition for simulation is shown in Table 1. Boundary surfaces were in Fig. 3. The time-dependent Backward Differentiation Formula (BDF) solver was used with the Parallel Sparse Direct Solver (PARDISO) to solve the equations of the deep-bed model. The mesh was generated using the finite element models with the 38.30 s meshing time. User-controlled methods and coarse types of mesh were selected to avoid the complexity of the simulation. The maximum and minimum element sizes were 0.274 and 0.0581, respectively. The maximum element growth rate was 1.4. Curvature factor and resolution of narrow regions 1 and 0.3, respectively. The absolute tolerance was 0.0001.

Table I. Initial and Boundary Conditions for Simulation

	Average inlet Airflow (m/s)	Inlet Air Temperature (℃)	Outlet Air Temperature (℃)	Inlet Air Relative humidity (%)	Outlet Air Relative humidity (%)	Temperature of surrounding (℃)
Initial	39.85	39.6	34	29.9	34.8	40.5
Final		51	39.2	21.2	28.1	43.3

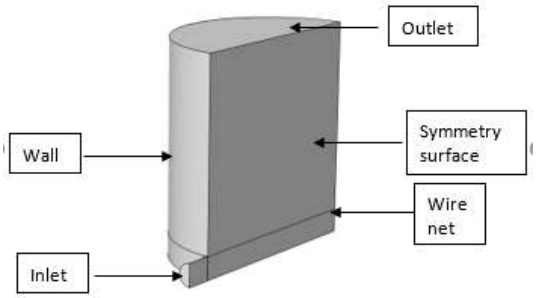

Fig. 3 Selected boundary condition of chamber for the simulation [13]

The performance of the simulation model was evaluated based on the relative error (RE) and mean relative deviation (MRD) based on the following equations [3]:

$$E = \frac{(M_j - \hat{M}_j)}{M_j} \times 100 \quad (7)$$

$$MRD = \left[\frac{1}{n}\sum_{j=1}^{n}\left(\frac{M_j - \hat{M}_j}{M_j}\right)^2\right]^{0.5} \times 100 \quad (8)$$

Where $M_j$and $\hat{M}_j$ indicate the j[th] experimental and predicted moisture content or temperature of air (dry basis), respectively, and n is the number of measurements in each experiment.

III. RESULTS AND DISCUSSION

In this simulation study, some major parameters of the drying air were analyzed within the chamber on the COMSOL Multiphysics interface. In addition, 3D CFD simulation was conducted to predict the airflow distribution because the result of a 2D simulation would not represent the real problem, as discussed by Misha [18]. The result is implemented at Intel® Core™ i3-3110M CPU @ 2.40GHz, 8.00 GB RAM, and 64-bit operating system.

Experimental results are illustrated in Fig. 4. Temperature and relative humidity showed the same pattern of changes in each layer. Minimum and maximum temperatures were 33.4℃ and 39.5℃. Even though relative humidity changed between 25% to 39%, the higher moisture concentration was observed near to the dryer wall. Overall, the drying chamber's mean temperature and relative humidity gradient were approximately 36.45 °C and 32%, which is a reasonable value for heat pump drying conditions.

A. CFD simulation of velocity fields in the dryer.

Fig. 5 below is displayed the velocity field inside a middle vertical plane (side view) in the dryer. The velocity decreases towards the exit section, the outlet. According to the simulation data, a stable air flow condition was achieved within 2 minutes.

As shown in Fig. 5, the airflow velocity is unevenly distributed at the bottom of the chamber. When the air moves upward, velocity is evenly distributed in each direction. The color legend shows the magnitude of the velocity field. Even though the inlet velocity field was around 39.6 ms^{-1}, the velocity at the top of the chamber was 1.0 ms^{-1}.

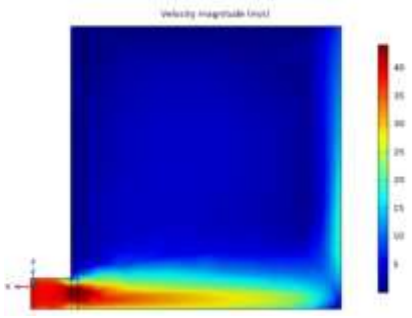

Fig. 5 Velocity distribution in a vertical cross section of chamber

B. CFD simulation of temperature distribution in the drying chamber.

The temperature profile's uniformity of hot air flow distribution in the drying chamber can be assessed from cross section of the drying chamber. Through the several plans, the closest plane of the outlet of the drying chamber presented a poor zone (Figure 6(a)) compared to the bottom plan (Figure 6(c)) in terms of hot air distribution due to its location and the effect of the blower. The temperature contours of each layer in the dryer are presented in Fig. 6(a-c).

Fig. 7 illustrates the distribution of temperatures inside the drying chamber. The vertical plane is homogeneous, except the bottom of the drying chamber (air inlet), and near the wall opposite the inlet, higher temperatures are obtained. The hot air temperature from the inlet was changed from 39.6°C to 51°C during the drying period. It was found that the average temperature at the three layers of simulation results was in the range of 34.85 °C to 39.85 °C.

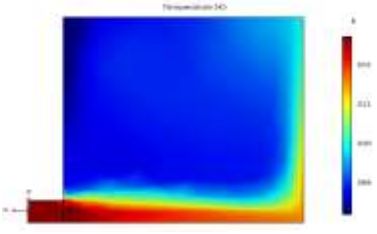

Fig. 6 Temperature distribution in a vertical cross section of chamber

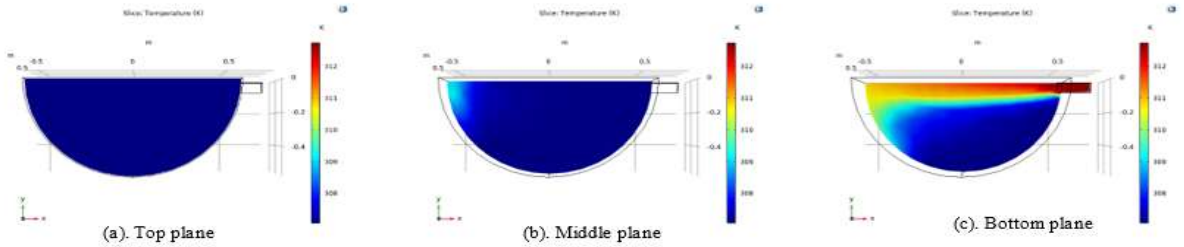

Fig. 6 Temperature distribution of each layer in chamber

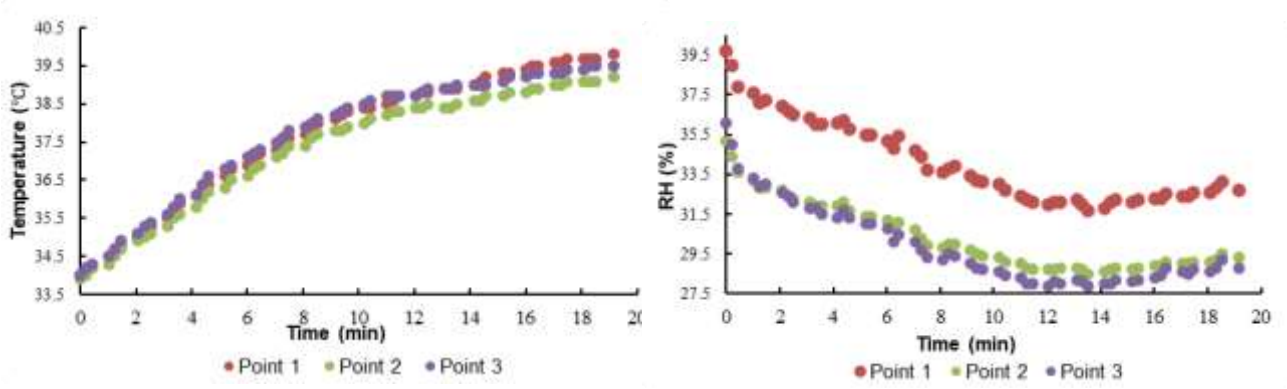

(a). Experimental results in Temperature and relative humidity profile of 75 cm depth layer

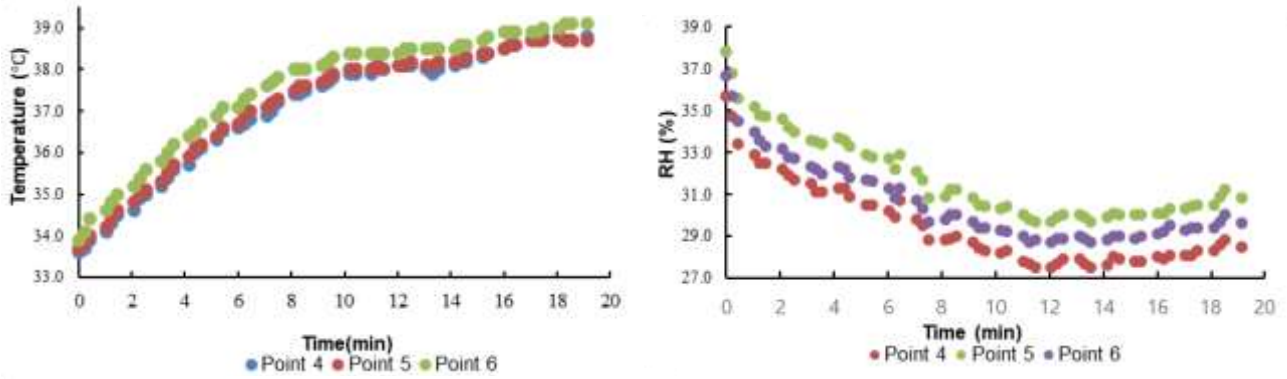

(b). Experimental results in Temperature and relative humidity profile of 45 cm depth layer

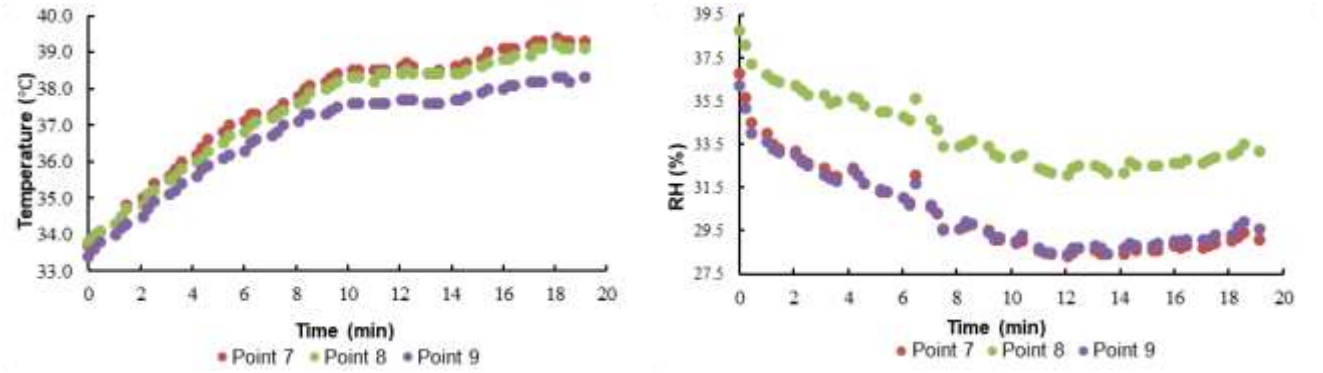

(c). Experimental results in Temperature and relative humidity profile of 15 cm depth layer

Fig. 4 Experimental results of Temperature and Relative humidity profile in dryer for 20 min drying period

C. CFD simulation of relative humidity distribution in the dryer.

Fig. 8 shows the moisture content distribution with the 5 minutes drying time interval and indicates amore significant moisture gradient mainly near the dryer wall. It could be a reason for achieving uneven drying conditions of a deep bed.

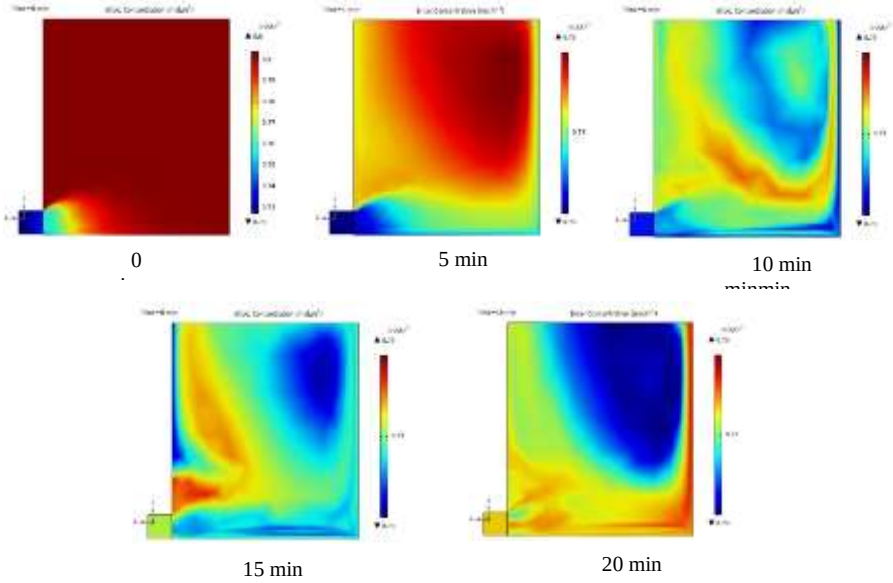

Fig. 8 Relative humidity distribution in a vertical cross section of chamber with the 5 min time interval

D. Results of CFD simulation

Table II. The Results of Validation Test for Predictions of Air Temperature and Air Relative Humidity.

	Air Temperature (℃)		Air Relative Humidity (%)	
	Relative error (%)	Mean relative deviation (%)	Relative error (%)	Mean relative deviation (%)
A_2	-0.192	0.447	6.286	8.93
A_3	-0.611	0.717	-4.713	8.15
A_4	-0.272	0.463	-6.507	9.59
A_5	-1.840	1.904	-7.868	10.68
A_6	-1.371	1.453	-0.203	6.65
A_7	-0.623	0.772	-4.019	7.83
A_8	-1.678	1.764	-5.021	8.82
A_9	-1.047	1.156	6.662	8.67
A_{10}	-2.857	2.879	-4.648	8.26

In this experiment, inlet, air temperature, and relative humidity were changed range from 39.6℃ - 51 ℃ and 29.9% - 21 %, respectively, while the air velocity in inlet was constant at the speed of 39.85 ms^{-1}. Table 2 shows the results of validation tests for predictions of air temperature and air relative humidity. Compared with experimental data, the mean relative deviation (MRD) values for predicting drying air temperature and relative humidity were less than 2.8 % and 10.68%, respectively. Previous researchers have accepted their models with a less than 15% error as an appropriate degree of agreement between simulation and experimental data [1, 12, 17, 20, 23]. The lowest and the highest values for MRD are 0.447% and 10.68%, respectively, whereas the minimum and maximum obtained values for RE are -0.192% and 6.662%, respectively Therefore, the results showed that the model could predict drying air temperature and humidity with reasonable accuracy.

The errors of predicting drying parameters could be due to making the assumptions, actual performance of the dryer, errors when selecting the initial parameters of the simulation.

This study has potential limitations. At this point we only considered the temperature, relative humidity and stable velocity field for the input airflow, future research work should be done for different drying conditions to find the optimization of the process. Moreover, we could not consider the airflow density changes during the time due to complexity of research.

IV. CONCLUSION

In this article, the commercial CFD software COMSOL Multiphysics was expanded to simulate the heat pump dryer. The simulation results were compared with some experimental data of drying. The obtained values of mean relative deviation (MRD), relative error (RE) for air temperature prediction, and humidity were less than 7.8%., ±1.8% and 10.6%., ±2.8%., respectively. The results revealed that the CFD model had a good performance for predicting air temperature and moisture content and it visualize the

temperature and moisture profile throughout the drying period. It could be used to decide when optimizing the drying system. Further work is needed to equip commercial CFD software with the different air velocities, different levels of the inlet air mass, and temperature.

V. NOMENCLATURE

T	Air temperature (K)
CFD	Computational Fluid Dynamic
MRD	Mean relative deviation (%)
RE	Relative error (%)
RH	Relative humidity (%)
Q	Heat Energy (W/m^3)
I	Fluid enthalpy (J/kg)
P	Pressure (Pa)
U	Velocity vector (m/s)
F	Volume force vector (N/m^3)
D	Diffusion coefficient
X	Position in the chamber (m)
C	Vapor concentration (mol/m^3)
Q_p	Work done by pressure changes (W)
Q_{vd}	Viscous dissipation in the fluid (W/m^3)
μ	Dynamic viscosity (Pa.s)
t	Time (s)
c_p	Specific heat capacity in a constant pressure (J/Kg.K)
Q_{br}	Mass sink source (kg/m^3. s)
Greek letters	
ρ	Density of fluid (kg/m^3)
τ	Viscos stress tensor (Pa)
α_p	Coefficient of thermal expansion (1/K)
q	Heat flux by conduction (W/m^2)
p	Density (kg/m^3)
u	Inflow velocity vector (m/s)

REFERENCES

[1] Dimitriadis, A. N., & Akritidis, C. B. (2004). A model to simulate chopped alfalfa drying in a fixed deep bed. Drying Technol., 22(3), 479-490. https://doi.org/10.1081/DRT-120029994

[2] ElGamal, R. A., Kishk, S. S., & ElMasry, G. M. (2017). Validation of CFD models for the deep bed drying of rice using thermal imaging. Biosyst. Eng., 161, 135-144. https://doi.org/10.1016/j.biosystemseng.2017.06.018

[3] ElGamal, R., Ronsse, F., & Pieters, J. (2013). Modeling deep-bed grain drying using Comsol Multiphysics. Proc. COMSOL Conf.

[4] Ficarella, A., Perago, A., Starace, G., & Laforgia, D. (2003). Thermo-fluid-dynamic investigation of a dryer, using numerical and experimental approach. Journal of food engineering, 59(4), 413-420.https://doi.org/10.1016/S0260-8774(02)00500-9

[5] Getahun, E., Vanierschot, M., Gabbiye, N., Delele, M. A., Workneh, S., & Gebrehiwot, M. (2019). Computational fluid dynamic modeling and simulation of red chili solar cabinet dryer. Proc. 4th Int. Conf. on Advancements of Science and Technology. https://doi.org/10.1007/978-3-030-43690-2_45.

[6] Ghiaus, A. G., & Gavriliuc, R. (2007). Simulation of air flow and dehydration process in tray drying systems. UPB Sci. Bull. (69), 41-50.

[7] Goh, L. J., Othman, M. Y., Mat, S., Ruslan, H., & Sopian, K. (2011). Review of heat pump systems for drying application. Renewable and Sustainable Energy Reviews, 15(9), 4788-4796. https://doi.org/10.1016/j.rser.2011.07.072.

[8] Harchegani, M. T., Moheb, A., Sadeghi, M., Tohidi, M., & Naghavi, Z. (2012). Experimental study of operating parameters affecting deep-bed drying kinetics of rough rice and comparing with a non-equalibrium mathematical model: Agric. Eng. Int.: CIGR J., 14(4), 195-202.

[9] Horikiri, K., Yao, Y., & Yao, J. (2011). Numerical simulation of convective airflow in an empty room. International Journal of Energy and Environment, 5(1), 574-581.

[10] Jamaleddine, T. J., and Ray, M. B (2010). Application of computational fluid dynamics for simulation of drying processes: A review. Drying technology,28(2),120-14. https://doi.org/10.1080/07373930903517458

[11] Janjai, S., Srisittipokakun, N., & Bala, B. K. (2008). Experimental and modelling performances of a roof-integrated solar drying system for drying herbs and spices. Energy, 33(1), 91-103.https://doi.org/10.1016/j.energy.2007.08.009

[12] Kalbasi, M. (2003). Heat and moisture transfer model for onion drying. Drying Technol., 21(8), 1575-1584. https://doi.org/10.1081/DRT-120024492

[13] Kavindi, M. R., Amaratunga, K. S. P., Ekanayake, E. M. C., Fernando, A. J., & Abesinghe, A. M. S. K. (2021). CFD Simulation of Airflow Distribution in a Heat Pump Assisted Deep-Bed Paddy Dryer. In Applied Engineering in Agriculture, 38(1): 1-8, doi: 10.13031/aea.14483.

[14] Kumar, A., Pramanik, S., & Mishra, M. (2016). COMSOL Multiphysics modeling in darcian and non-darcian porous media. In Proceedings of the 2016 COMSOL Conference, Bangalore, India (pp. 20-21).

[15] Liu, H., Yousaf, K., Chen, K., Fan, R., Liu, J., & Soomro, S. A. (2018). Design and thermal analysis of an air source heat pump dryer for food drying. Sustainability, 10(9), 3216. https://doi.org/10.3390/su10093216

[16] Mabrouk, S. B., Khiari, B., & Sassi, M. (2006). Modelling of heat and mass transfer in a tunnel dryer. Applied thermal engineering, 26(17-18), 2110-2118. https://doi.org/10.1016/j.applthermaleng.2006.04.007

[17] Madhiyanon, T., Soponronnarit, S., & Tia, W. (2001). Industrial scale prototype of continuous spouted bed paddy dryer. Drying Technol., 19(1), 207-216. https://doi.org/10.1081/DRT100001362

[18] Misha, S., Mat, S., Rosli, M. A., Ruslan, M. H., Sopian, K., & Salleh, E. (2015) Simulation of air flow distribution in a tray dryer by CFD. Proc. 10th Int. Conf. on Energy & Environment. Recent Advances in Renewable Energy Sources, (pp. 126-135)

[19] Noh, A., Mat, S.., & Ruslan, M. H. (2020). CFD Simulation of Temperature and Air Flow Distribution Inside Industrial Scale Solar Dryer. Journal of Advanced Research in Fluid Mechanics and Thermal Sciences, 45(1), 156–164. Retrieved from https://akademiabaru.com/submit/index.php/arfmts/article/view/2192

[20] Park, K. J., Vohnikova, Z., & Brod, F. P. R. (2002). Evaluation of drying parameters and desorption isotherms of garden mint leaves (Mentha crispa L.). J. Food Eng., 51(3), 193-199. https://doi.org/10.1016/S0260-8774(01)00055-3

[21] Patel, K. K., & Kar, A. (2012). Heat pump assisted drying of agricultural produce: An overview. J. Food Sci. Technol., 49(2), 142-160. https://doi.org/10.1007/s13197-011-0334-z

[22] Ranjbaran, M., Emadi, B., & Zare, D. (2014). CFD Simulation of deep-bed paddy drying process and performance. Drying Technol., 32(8), 919-934. https://doi.org/10.1080/07373937.2013.875561

[23] Sitompul, J. P., Istadi, & Widiasa, I. N. (2001). Modeling and simulation of deep-bed grain dryers. Drying Technol., 19(2), 269-280. https://doi.org/10.1081/DRT-10010290

[24] Salehi, F. (2021). Recent applications of heat pump dryer for drying of fruit crops: A review. Int. J. Fruit Sci., 21(1), 546-

555.https://doi.org/10.1080/15538362.2021.1911746
[25] Woo, M. W., Daud, W. R. W., Mujumdar, A. S., Wu, Z., Meor Talib, M. Z., & Tasirin, S. M. (2008). CFD evaluation of droplet drying models in a spray dryer fitted with a rotary atomizer. Drying Technology, 26(10), 1180-1198.https://doi.org/10.1080/07373930802306953
[26] Zare, D., Minaei, S., Mohamad Zadeh, M., & Khoshtaghaza, M. H. (2006). Computer simulation of rough rice drying in a batch dryer. Energy Conversion Manag., 47(18), 3241-3254. https://doi.org/10.1016/j.enconman.2006.02.021